PHYSICAL REVIEW B **88**, 195202 (2013)

Picosecond real-space imaging of electron spin diffusion in GaAs

T. Henn, T. Kiessling,* W. Ossau, and L. W. Molenkamp
Physikalisches Institut (EP3), Universität Würzburg, 97074 Würzburg, Germany

D. Reuter and A. D. Wieck
Institut für angewandte Festkörperphysik, Ruhr-Universität Bochum, 44780 Bochum, Germany

(Received 3 September 2013; published 12 November 2013)

We use time-resolved two-color Kerr microscopy to study low-temperature electron spin diffusion in bulk GaAs with high spatial and temporal resolution. This method enables direct real-space imaging of the advancing spread of an optically excited electron spin packet by spin diffusion. We observe a high initial expansion rate of the spin packet, which is strongly reduced with increasing time. Comparison with continuous-wave Kerr spectroscopy demonstrates that this decrease is caused by the influence of the transient cooling of hot photocarriers on the electron spin diffusion coefficient.

DOI: 10.1103/PhysRevB.88.195202 PACS number(s): 72.25.Dc, 72.25.Fe, 85.75.−d, 72.25.Rb

I. INTRODUCTION

The future implementation of spin-based electronic (spintronic) devices relies on the ability to precisely control the storage, manipulation, and transport of spin coherence in solid state systems.[1,2] Significant progress has been achieved regarding the realization of long-time storage and manipulation of electron spin polarization down to the single-spin level.[3,4] However, a consistent understanding of electron spin transport in semiconductors has not been reached yet.

Spin-sensitive optical pump-probe spectroscopy indicates strong deviations between low-temperature charge carrier and electron spin transport. A particularly remarkable result is the repeated observation that the spin diffusion coefficient D_s exceeds the charge diffusivity D_c by an order of magnitude in bulk GaAs at low temperatures.[5–7] This finding contradicts the theoretical prediction that D_s is reduced with respect to D_c by Coulomb interaction.[8]

Cundiff *et al.* were among the first to propose that the enhancement of D_s observed under optical excitation results from photocarrier heating.[9] The significance of pump-induced electron heating for the diffusion of photoexcited carriers has been understood for a long time in the context of exciton transport in quantum wells.[10,11] However, such hot electron effects have been neglected in the interpretation of early results on low-temperature electron spin diffusion obtained by magneto-optical Kerr (MOKE) microscopy and transient spin grating measurements.

The present work is the first to *directly* measure the influence of photocarrier heating on electron spin diffusion. We report on real-space imaging of electron spin diffusion in bulk GaAs with picosecond time and micron spatial resolution. We study the temporal evolution of the spread of an optically excited electron spin packet by spin diffusion. We directly measure the time-dependence of the electron spin diffusion coefficient from the momentary expansion rate of the spin packet. We observed a high initial expansion rate of the spin packet. For low lattice temperatures this expansion rate is strongly reduced with increasing time, reflecting a transient decrease of the spin diffusion coefficient. We show that this decrease of D_s is caused by the influence of cooling of hot photocarriers on the electron spin diffusion coefficient.

II. SAMPLE AND EXPERIMENTAL SETUP

We investigate the lateral in-plane diffusion of the spin polarization of electrons whose motion is constricted to a 1-μm-thick MBE-grown n-GaAs epilayer[12] with a room-temperature electron density $n = 1.4 \times 10^{16}$ cm^{-3} and electron mobility $\mu_c \approx 5500$ cm^2 v^{-1} s^{-1}.

The sample is mounted strain-free on the cold finger of an optical cryostat. A calibrated resonant-tunneling diode (RTD) sensor is attached to the backside of the sample holder for accurate measurements of the sample temperature which can be varied between 8 K and 300 K.

The Kerr microscopy setup shown in Fig. 1(a) allows for both continuous wave (cw) excitation and time-resolved spectroscopy. A detailed description of the setup is provided in Ref. 13. In brief, two independent, continuously tunable Ti:sapphire lasers provide the pump and probe laser beams for cw measurements. For time-resolved two-color spectroscopy, we employ a pulsed ultrafast white light supercontinuum source. The output of a high power mode-locked infrared laser system ($\lambda \approx 1040$ nm, pulse length $\lesssim$300 fs, 36.4 MHz repetition rate) is coupled into a tapered fiber with a waist diameter of $\approx$4 μm. A typical output spectrum resulting from nonlinear supercontinuum generation in the fiber[14,15] is shown in Fig. 1(b). After exiting the fiber the laser is collimated by a microscope objective. Pulsed pump and probe beams are derived from the white light supercontinuum by dividing the laser in two components by a broadband antireflection-coated beamsplitter and performing individual spectral filtering.

Tunable spectral filtering of the probe laser is achieved by dispersing the supercontinuum with a prism and passing the output of the prism through a pair of lenses arranged in confocal geometry. The desired wavelength component is selected with a 50-μm pinhole placed in the common focal plane of the lens pair. Variation of the position of the first lens results in a continuously tunable probe laser spectrum with a FWHM $\lesssim$30 Å for photon energies close to the GaAs

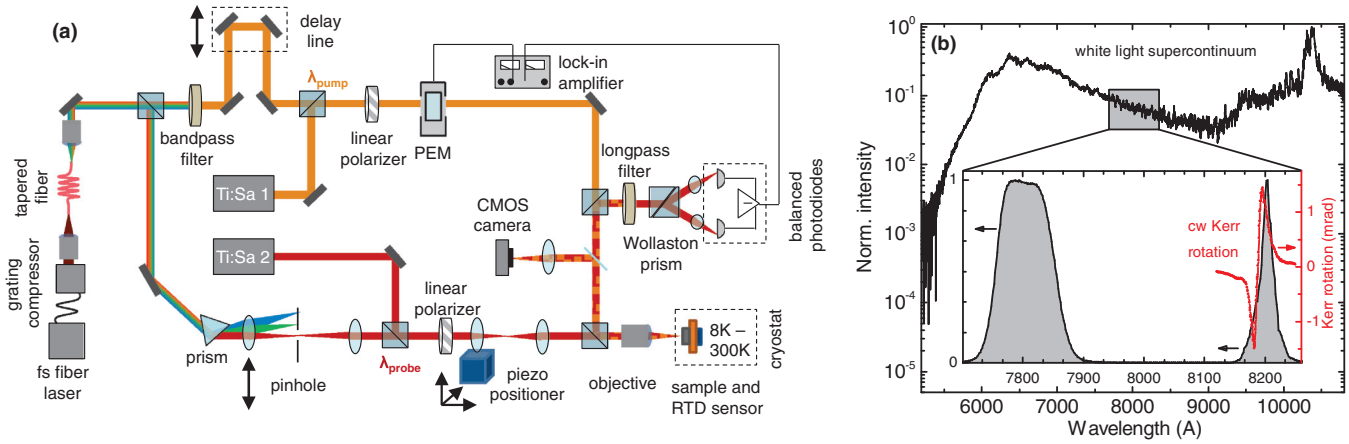

FIG. 1. (Color online) (a) Schematic of the two-color pump-probe scanning Kerr microscopy setup. (b) White light supercontinuum generated by passing an infrared fs laser pulse through a tapered fiber. (Inset) Normalized intensity spectra of the pulsed pump and probe lasers after spectral filtering (left axis, black). The spectral range of the inset is indicated by the gray box. The spectral dependence of the cw Kerr rotation $\theta_K(\lambda_{\text{probe}})$ measured at $T_L = 8$ K for excitation at $\lambda_{\text{pump}} = 7800$ Å is shown on the right axis (red).

band gap. The pump laser is spectrally filtered by passing the supercontinuum through a dielectric bandpass filter. This results in an intensity spectrum centered at 7800 Å with a FWHM of 100 Å shown in Fig. 1(b). A mechanical delay line is used to introduce a variable delay Δt between the pump and probe pulse. The overall temporal resolution of the setup is well below 5 ps as evidenced by the quantitative analysis of very fast rises observed in Kerr rotation transients.[13]

For pulsed and cw measurements the polarization of the pump laser is periodically modulated at 50.1 khZ between σ^+ and σ^- circular polarization by a photoelastic modulator (PEM). Electrons with a net spin polarization S_z along the sample normal are locally excited by the pump laser beam.[16] A balanced photodetector in combination with a standard lock-in detection scheme[17] is used to measure the photoinduced Kerr rotation $\theta_K \sim S_z$, which is imposed on the second, linearly polarized probe beam upon reflection from the sample surface.[18]

Both laser beams are focused on the sample surface at normal incidence with an apochromatic microscope objective (NA = 0.42, $f = 4$ mm). For cw excitation, the $(1/e)$ half-widths of the Gaussian pump and probe spots are 0.7 μm and 1.2 μm as determined from CMOS camera images. By convolution, this results in a net optical resolution of 1.4 μm. For pulsed excitation we achieve a slightly lower resolution of $\sigma_0 \approx 2.2$ μm. Lateral scanning of the probe with respect to the pump spot is accomplished by varying the relative position of two aspheric lenses in confocal geometry by a piezopositioner.

For all cw excitation measurements, the pump wavelength is set to 7800 Å and a pump power of 10 μW is used. The probe power is 50 μW and the probe wavelength is set to 8210 Å.

For time-resolved measurements, the time-averaged pump and probe power are 6 and 12 μW, respectively. The wavelength of the pulsed probe laser is tuned to the E_0 excitonic Kerr resonance and chosen such that the observed Kerr rotation is maximal. Figure 1(b) shows the pulsed probe laser spectrum used for measurements at a lattice temperature $T_L = 8$ K together with the corresponding cw Kerr spectrum $\theta_K(\lambda_{\text{probe}})$. We have verified that the results presented in this work do not change under variation of the probe laser wavelength.

Time-resolved imaging of the electron spin polarization is achieved by repeatedly raster scanning the probe with respect to the pump spot and measuring the local Kerr rotation $\theta_K(r) \sim S_z(r)$. Systematic variation of the pump-probe delay Δt then directly maps the time evolution of the spin polarization $S_z(\Delta t, r)$.

III. RESULTS AND DISCUSSION

A. Time-dependent electron spin diffusion model

The quasi-two-dimensional expansion of an electron spin packet in the thin GaAs epilayer plane following a short excitation pulse is governed by the diffusion equation:

$$\frac{\partial S_z}{\partial t} = D_s \frac{1}{r}\frac{\partial}{\partial r}\left(r\frac{\partial S_z}{\partial r}\right) - \frac{S_z}{\tau_s}. \tag{1}$$

Here, τ_s denotes the spin relaxation time and r is the radial distance measured from the pump spot center. For a Gaussian pump spot, the time evolution of the spin polarization after a short excitation pulse is[10,19,20]

$$S_z(\Delta t, r) = \frac{\sigma_0^2 S_{z,0}}{\sigma_0^2 + 4D_s\Delta t}\exp\left(\frac{-r^2}{w_s^2}\right)\exp\left(\frac{-\Delta t}{\tau_s}\right) \tag{2}$$

with a time-dependent squared $(1/e)$ half-width

$$w_s^2 = \sigma_0^2 + 4D_s\Delta t \tag{3}$$

and an initial Gaussian $(1/e)$ half-width σ_0. From Eq. (2), it is obvious that diffusion leads to a nonexponential decay of the spin polarization $S_z(\Delta t, r = 0\ \mu\text{m})$ at the pump spot center.

For cw excitation, the shape of the stationary spin polarization profile results from the combined action of spin relaxation and diffusion.[7,21] Steady-state Kerr microscopy therefore relies on complementary measurements of the spin relaxation time for the determination of spin diffusion

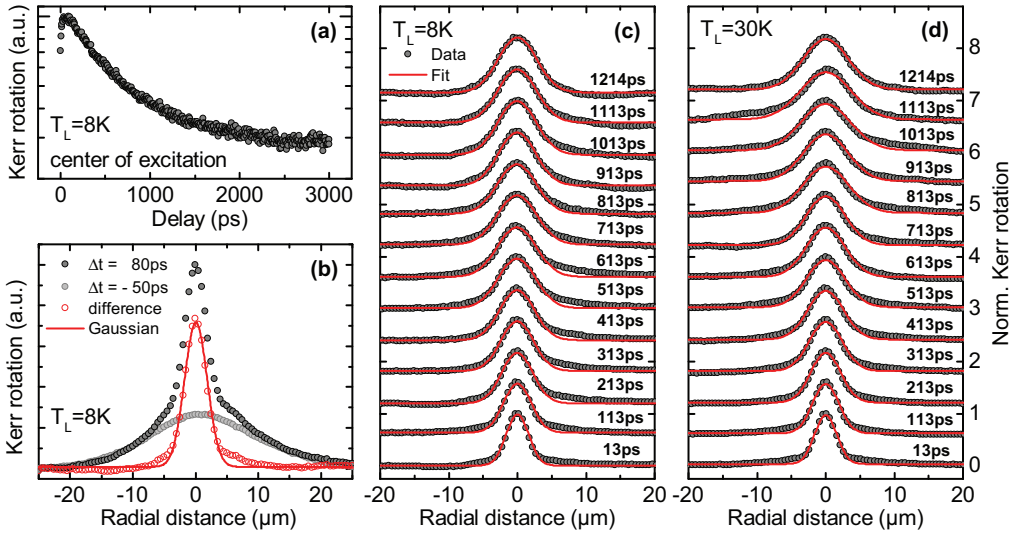

FIG. 2. (Color online) (a) Transient Kerr rotation $\theta_K(\Delta t, r = 0\ \mu\text{m})$ plotted on a logarithmic scale. The nonexponential decay reflects the influence of diffusion on the spin dynamics (see text). (b) Lateral Kerr rotation profiles for delays $\Delta t = -50$ ps (light gray markers) and $\Delta t = 80$ ps (dark gray markers) at $T_L = 8$ K. The non-Gaussian spin profile observed at positive delay times is a superposition of the currently injected spin packet with previous-pulse contributions. The profile resulting from subtraction of the previous-pulse contributions (red markers) is shown together with a Gaussian fit (solid red line). (c,d) Lateral spin polarization profiles at $T_L = 8$ and 30 K (gray markers) for increasing delays (bottom to top) and Gaussian fits (solid lines). The delay Δt is indicated above the respective curve. From each profile, the previous-pulse contributions are subtracted. Profiles are normalized and shifted vertically.

coefficients.[7,22] By contrast, for short-pulsed excitation, spin propagation, and relaxation are completely decoupled. The shape of the spin polarization profile is solely determined by the action of diffusion while spin relaxation only modifies the overall amplitude of the spin packet. Unlike cw spectroscopy, time-resolved Kerr microscopy therefore allows for a direct measurement of the spin diffusion coefficient.

For a *constant* spin diffusivity independent of Δt we expect from Eq. (3) a *linear* dependence of w_s^2 on the pump-probe delay Δt with a slope of $4D_s$. Measurement of the Gaussian width $w_s(\Delta t)$ of the spin packet therefore directly reveals the spin diffusivity

$$D_s = \frac{1}{4}\frac{\partial}{\partial \Delta t}\left(w_s^2(\Delta t)\right). \tag{4}$$

We note that for a Gaussian spin packet (4) is also valid for a time-dependent spin diffusion coefficient where $D_s(\Delta t)$ is determined from the momentary slope of the tangent to the $w_s^2(\Delta t)$ curve.[10]

B. Time-resolved electron spin diffusion spectroscopy

We study time-resolved lateral electron spin diffusion for sample temperatures $T_L = 8$, 20 and 30 K. For each T_L, we measure line cuts of the electron spin polarization profile $S_z(r)$ through the pump spot center for increasing pump-probe delays Δt between -100 and 1350 ps.

A typical time trace of the local spin polarization $S_z(\Delta t, r = 0\ \mu\text{m})$ additionally measured at $T_L = 8$ K for delays up to 3000 ps is shown in Fig. 2(a) on a logarithmic scale. The strong influence of diffusion on the decay of $S_z(\Delta t, r = 0\ \mu\text{m})$ expected from Eq. (2) is evident from the deviation of the experimental data from a straight line.

In Fig. 2(b), we show the spin polarization profile $S_z(r)$ measured at $T_L = 8$ K for a short delay $\Delta t = 80$ ps. The profile of the spin packet clearly is non-Gaussian. This is a result of the long spin spin relaxation time $\tau_s \approx 170$ ns at low temperatures [see Fig. 4(b)] and the relatively low spin diffusivity of the sample. The spin polarization excited by the previous pump pulses does not completely decay within the 27.5 ns pulse-to-pulse interval of our supercontinuum source. This is evidenced by the second $S_z(r)$ profile shown in Fig. 2(b) measured at a short negative delay $\Delta t = -50$ ps before the arrival of the corresponding pump pulse. We observe a substantial remanent spin polarization excited by previous pump pulses, which strongly decreases for rising lattice temperatures and completely vanishes at $T_L = 30$ K. This reflects enhanced diffusion and a strong decrease of τ_s with increasing temperature [compare Fig. 4(b)].

We limit our analysis to the contribution of the spin polarization resulting from the excitation by a single pump pulse. Because of the linearity of the diffusion Eq. (1) the momentary spin polarization is a superposition of the contributions of all previous excitation pulses. On the short time scale of our observation window of 1350 ps and for the comparatively long pulse-to-pulse interval of our experiment, the spin profile resulting from the previous excitation pulses is virtually stationary. Following Ref. 6, we therefore subtract the previous-pulse contribution profile measured at short negative delays of -50 ps from each spin polarization profile $S_z(\Delta t, r)$. The resulting single-pulse profiles then are Gaussians as shown in Fig. 2(b) where we exemplarily compare the experimental data for $\Delta t = 80$ ps with a Gaussian fit. An alternative technique to reduce repetition-rate artifacts is the suppression of previous-pulse contributions by destructive spin interference[23] by application of a small in-plane magnetic field

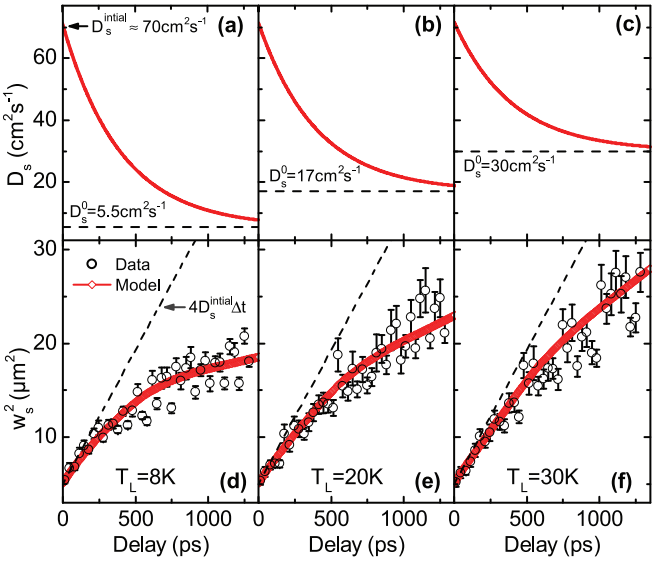

FIG. 3. (Color online) (a)–(c) Time-dependent spin diffusion coefficient $D_s(\Delta t)$ used for transient finite element method (FEM) simulations (see text and below). The dashed lines indicate the intrinsic spin diffusivity D_s^0 which was obtained for the respective T_L from independent cw measurements. (d)–(f) Measured time evolution of the squared Gaussian width $w_s^2(\Delta t)$ of the electron spin packet (black circles) for $T_L = 8$, 20 and 30 K. The dashed lines indicate the expansion of a spin packet for a constant diffusion coefficient $D_s^{\text{initial}} \approx 70$ cm^2 s^{-1}. Also shown is the results of the transient FEM simulation assuming a time-dependent spin diffusion coefficient (red diamonds, see text).

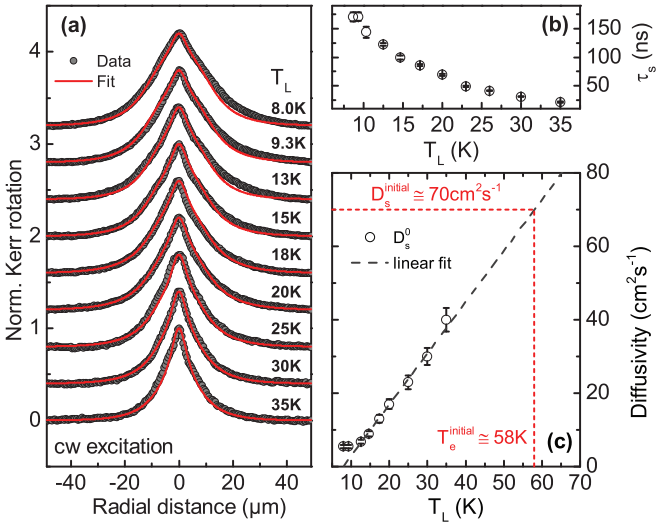

FIG. 4. (Color online) (a) Lateral steady-state electron spin polarization profiles obtained for cw excitation at T_L ranging from 8 to 35 K (gray markers). Solid red lines are best fits from a modified diffusion model (see text). (b) Temperature dependence of the spin relaxation time $\tau_s(T_L)$. (c) Intrinsic spin diffusivity $D_s^0(T_L)$ (gray markers). The dashed gray line is a linear fit for $T_L \geqslant 12$ K. Red short dashed lines indicate the initial diffusivity and effective temperature of the spin packet at $\Delta t = 0$ ps (see text).

of $\approx$1 mT. We have verified that within experimental resolution both methods yield identical results for the following analysis.

Time traces of single-pulse spin polarization profiles $S_z(\Delta t, r)$ resulting from the above procedure are shown in Figs. 2(c) and 2(d) together with Gaussian fits for $T_L = 8$ and 30 K. The shape of the spin packets remains Gaussian for all examined times. For the shortest delay of 13 ps the $(1/e)$ half-width of the spin packet coincides with our optical resolution $\sigma_0 \approx 2.2$ μm. The diffusive spreading of the spin packet with increasing delay is clearly observable for both lattice temperatures. Careful inspection of Figs. 2(c) and 2(d) for long delays further reveals a stronger increase of the Gaussian width at high lattice temperature. This reflects the expected increase of the spin diffusivity with rising temperature.[22]

In Figs. 3(d)–3(f), we plot $w_s^2(\Delta t)$ for increasing T_L which we obtained from the Gaussian fits of the single-pulse spin polarization profiles. For all examined lattice temperatures we observe a strong deviation of $w_s^2(\Delta t)$ from the linear dependence on Δt, which is expected for a constant spin diffusivity D_s. With increasing time the $w_s^2(\Delta t)$ curves are *sublinear*, reflecting a *transient decrease of the spin diffusivity* $D_s(\Delta t)$. This transient decrease is strongest for $T_L = 8$ K and becomes less pronounced with increasing lattice temperature.

In contrast, we find that for all examined temperatures T_L the expansion during the first $\approx$100 ps is well described by the same diffusion coefficient $D_s^{\text{initial}} \approx 70$ cm^2 s^{-1} as indicated by dashed lines. For long delays $\Delta t \gtrsim 800$ ps, the expansion is quasilinear with Δt, indicating that $D_s(\Delta t)$ has approached a respective equilibrium value, which is found to increase with T_L.

In the remaining part of this manuscript, we will demonstrate that the observed decrease of $D_s(\Delta t)$ is consistently explained by considering the influence of the transient cooling of hot photocarriers on the spin diffusion coefficient: The $\lambda_{\text{pump}} \approx 7800$ Å pump pulse excites photoelectrons with a mean excess energy of $E_{\text{ex}} \approx 60$ meV.[24] This deposition of excess energy in the electron system leads to a strong heating of the electrons and results in an electron temperature T_e, which can significantly exceed the lattice temperature T_L.[25,26] Owing to the high initial kinetic energy of the spin-polarized electrons the spin diffusion coefficient will be strongly enhanced for short delays. For increasing Δt energy relaxation of the hot carriers takes place. This leads to the observed decrease of $D_s(\Delta t)$ down to the intrinsic value $D_s^0(T_L)$ for the respective lattice temperature.

C. Time-dependent hot carrier effects on electron spin diffusion

We first use cw Kerr microscopy to determine this intrinsic temperature dependence of the spin diffusion coefficient. In Fig. 4(a), we show lateral steady-state spin polarization profiles for increasing lattice temperatures together with best fits derived from a diffusion model. A detailed description of the cw measurements and the diffusion model is given in Appendix. From these fits, we obtain the temperature dependence $D_s^0(T_L)$, which is shown in Fig. 4(c). We find that $D_s^0(T_L)$ monotonically increases with rising temperature. For $T_L \geqslant 12$ K, we observe that this increase of the spin diffusivity is approximately proportional to the lattice temperature, i.e., $D_s^0 \sim T_L$.

We now use this $D_s^0(T_L)$ dependence for the interpretation of our time-resolved measurements. We first consider the very fast initial expansion of the electron spin packet. For $\Delta t \lesssim 100$ ps, we found that the expansion rate is independent of the lattice temperature and corresponds to a spin diffusivity $D_s^{\text{initial}} \approx 70\ \text{cm}^2\,\text{s}^{-1}$.

Comparison with the intrinsic temperature dependence of the spin diffusivity $D_s^0(T_L)$ allows for an estimation of the initial photocarrier temperature. From a linear extrapolation of $D_s^0(T_L)$ for $T_L \geqslant 12$ K shown in Fig. 4(c), we can estimate an initial electron temperature $T_e^{\text{initial}} \approx 58$ K for very short delays $\Delta t \lesssim 100$ ps after the pump pulse.[27] The observed value of D_s^{initial} is constant for all examined T_L because the initial kinetic energy of the electrons (and hence the initial electron temperature) is solely determined by the large excitation excess energy E_{ex} and does not depend on the lattice temperature.

Our estimate $T_e^{\text{initial}} \approx 58$ K is in good agreement with transient electron temperature calculations, which consider the energy relaxation by emission of optical and acoustical phonons.[26,28] For an initial photoelectron excess energy $E_{\text{ex}} = 60$ meV, we calculate an electron temperature $T_e = 56$ K for a delay $\Delta t = 13$ ps for which we measure the first $S_z(r)$ profile. Comparable initial electron temperatures have also been obtained previously from picosecond time-resolved photoluminescence spectroscopy studies of photocarrier thermalization in bulk GaAs.[29]

The temporal evolution of the electron temperature profile $T_e(\Delta t,r)$ following the short localized excitation by the pump pulse is governed by energy relaxation by emission of phonons, heat conduction in the electron system, and possibly impact ionization of donor-bound electrons.[26,28,30] An exact quantitative treatment of this problem is beyond the scope of this work. Instead, we characterize the electron spin packet by an effective temperature $\tilde{T}_{\text{eff}}$. In a first approximation, we model the thermal relaxation of the electrons constituting the spin packet by Newtonian cooling with a rate $(\partial \tilde{T}_{\text{eff}}/\partial \Delta t) \sim (\tilde{T}_{\text{eff}} - T_L)$, i.e., $\tilde{T}_{\text{eff}}$ will approach T_L exponentially for long delays.

Motivated by the linear dependence of D_s^0 on temperature observed in Fig. 4(c), we then approximate the transient spin diffusion coefficient by

$$D_s(\Delta t,T_L) = D_s^0(T_L)[1 + A_t \exp(-\Delta t/\tau_c)]. \qquad (5)$$

The cooling constant τ_c characterizes the time scale on which the effective temperature $\tilde{T}_{\text{eff}}$ of the spin packet decays to the respective lattice temperature T_L. Following the cooling of the spin packet, for increasing delay the spin diffusivity $D_s(\Delta t)$ approaches the equilibrium value D_s^0 for the respective lattice temperature T_L, which we independently determine from cw spectroscopy. The transient enhancement amplitude A_t is a measure for the influence of the high initial kinetic energy of the photocarriers on the spin diffusivity. It is determined by the boundary condition $D_s(\Delta t = 0\ \text{ps}) = D_s^{\text{initial}}$, leaving the cooling time constant τ_c as the only free parameter.

We use a transient finite element method (FEM) solver to obtain the solution of the spin diffusion Eq. (1) for the time-dependent spin diffusivity $D_s(\Delta t,T_L)$ described by Eq. (5). Excitation by the short pump pulse is modeled by a Gaussian source term $g(\Delta t,r) = g_0 \exp(-r^2/\sigma_0^2)\exp(-\Delta t^2/\tau_g^2)$. The spatial extent of the source term is determined by our optical resolution $\sigma_0 = 2.2\ \mu$m. A pulse length $\tau_g = 2$ ps is used in the simulations. For the spin relaxation time $\tau_s(T_L)$ we use the values shown in Fig. 4(b), which we independently obtained from standard cw Hanle-MOKE measurements. From the FEM solution of our model,we then extract the squared Gaussian $(1/e)$ half-width $w_s^2(\Delta t)$.[31]

Variation of τ_c and comparison of the numerical results with the experimental data allows us to determine the unknown cooling decay time. In Figs. 3(d)–3(f) we show the $w_s^2(\Delta t)$ curves obtained for $\tau_c = 400$ ps from our model together with the experimental data. Very similar cooling times have been observed previously in time-resolved exciton diffusion experiments for GaAs quantum wells.[10] For all examined lattice temperatures T_L we find good quantitative agreement between the experimental data and the numerical results for this value of τ_c. The resulting time-dependent spin diffusion coefficient $D_s(\Delta t)$ used for the respective calculation is shown in Figs. 3(a)–3(c). For comparison, we also show by dashed lines the intrinsic spin diffusivity D_s^0 for the respective lattice temperature, which is approached for long delays.

IV. CONCLUSIONS

In conclusion, we have used picosecond Kerr microscopy to image the expansion of optically excited electron spin packets by spin diffusion in bulk GaAs. The time-resolved measurement of the Gaussian width of the spin packet allows us for the first time to *directly* observe the influence of pump-induced photocarrier heating on electron spin diffusion. By comparison with accompanying cw Kerr microscopy measurements we are able to draw the following physical picture: For very short delays after the pump pulse, spin diffusion is very fast and the high initial diffusivity is solely determined by the initial kinetic energy of the photoexcited electrons. With increasing delay thermal relaxation of the hot photocarriers takes places. The cooling of the electron population down to the lattice temperature by both phonon emission and heat conduction in the electron system is found to happen on a time scale $\tau_c \approx 400$ ps. This transient reduction of the kinetic energy of the electrons is reflected by a strong decrease of the spin diffusion coefficient with increasing time. For long delays $\Delta t \gg \tau_c$, the influence of photocarrier heating vanishes. The expansion of the spin packet is then observed to take place with the rate expected from the intrinsic spin diffusion coefficient, which we independently determined from cw Kerr microscopy.

ACKNOWLEDGMENT

The authors gratefully acknowledge support by the DFG (SPP1285 OS98/9-3 and RE1507/3-3).

APPENDIX: STEADY-STATE ELECTRON SPIN DIFFUSION

We determine the intrinsic temperature dependence of the electron spin diffusion coefficient $D_s^0(T_L)$ from standard cw excitation Kerr microscopy.[7,22,32] We therefore measure line cuts of the steady-state spin polarization profile $S_z(r)$ for

T_L between 8 and 35 K, which are shown in Fig. 4(a). We employ a modified spin diffusion model to extract the intrinsic temperature dependence $D_s^0(T_L)$ from these line cuts.

The modified diffusion model is discussed in detail in Ref. 22. Similar to the transient case, optically excited steady-state spin diffusion is strongly influenced by pump-induced carrier heating. In the framework of the modified diffusion model, a local enhancement of the electron spin diffusivity close to the pump spot caused by hot photocarriers is considered by a spatially varying diffusion coefficient

$$D_s(r,T_L) = D_s^0(T_L)\left[1 + A_D \exp\left(-r^2/\sigma_D^2\right)\right]. \qquad \text{(A1)}$$

The magnitude of the local diffusion enhancement by carrier heating is characterized by the amplitude A_D. This enhancement amplitude is a measure for the temperature difference between the electron system and the lattice. The local enhancement of $D_s(r)$ decays on a length scale described by σ_D: $D_s(r)$ reaches the intrinsic value $D_s^0(T_L)$ for distances far away from the pump spot for which the electron system and the lattice are in thermal equilibrium.[30,33]

In analogy to Ref. 22, we use the finite element method (FEM) to numerically solve the modified steady-state electron spin diffusion equation[21,22,32]

$$\nabla_r(D_s(r)\nabla_r S_z(r)) - \tau_s^{-1} S_z(r) + g(r) = 0 \qquad \text{(A2)}$$

for the spatially varying diffusion coefficient $D_s(r)$. Optical spin excitation is modelled by a Gaussian source term $g(r) = g_0 \exp(-r^2/\Delta_g^2)$ with an $(1/e)$ half-width $\Delta_g = 1.4\ \mu$m (our optical resolution for cw excitation). The spin relaxation time $\tau_s(T_L)$ entering the diffusion model has been determined previously[22] by standard cw Hanle-MOKE spectroscopy[7,34] and is shown in Fig. 4(b).

The best fits obtained from the modified diffusion model are shown in Fig. 4(a). In accordance with Ref. 22, we find good agreement with the experimental data over the whole examined temperature range for an enhancement decay length $\sigma_D \approx 7\ \mu$m. The enhancement amplitude systematically decreases from $A_D \approx 6$ at $T_L = 8$ K to $A_D \approx 0.7$ at $T_L = 35$ K. This decrease demonstrates the vanishing influence of pump-induced electron heating at high lattice temperatures for which the electron system and the lattice approach thermal equilibrium.[30,35]

*tobias.kiessling@physik.uni-wuerzburg.de

[1] S. A. Wolf, D. D. Awschalom, R. A. Buhrman, J. M. Daughton, S. von Molnar, M. L. Roukes, A. Y. Chtchelkanova, and D. M. Treger, Science **294**, 1488 (2001).

[2] D. D. Awschalom and M. E. Flatté, Nat. Phys. **3**, 153 (2007).

[3] R. Hanson, J. R. Petta, S. Tarucha, and L. M. K. Vandersypen, Rev. Mod. Phys. **79**, 1217 (2007).

[4] R. Hanson and D. D. Awschalom, Nature **453**, 1043 (2008).

[5] R. I. Dzhioev, B. P. Zakharchenya, V. L. Korenev, and M. N. Stepanova, Phys. Solid State **39**, 1765 (1997).

[6] J. M. Kikkawa and D. D. Awschalom, Nature **397**, 139 (1999).

[7] M. Furis, D. L. Smith, S. Kos, E. S. Garlid, K. S. M. Reddy, C. J. Palmstrom, P. A. Crowell, and S. A. Crooker, New J. Phys. **9**, 347 (2007).

[8] I. D'Amico and G. Vignale, Eur. Phys. Lett. **55**, 566 (2001).

[9] S. G. Carter, Z. Chen, and S. T. Cundiff, Phys. Rev. Lett. **97**, 136602 (2006).

[10] H. W. Yoon, D. R. Wake, J. P. Wolfe, and H. Morkoç, Phys. Rev. B **46**, 13461 (1992).

[11] H. Zhao, S. Moehl, S. Wachter, and H. Kalt, Appl. Phys. Lett. **80**, 1391 (2002).

[12] The sample used in this work has been the subject of previous investigations. A detailed description of the sample structure is given in Refs. 22 and 23.

[13] T. Henn, T. Kiessling, W. Ossau, L. W. Molenkamp, K. Biermann, and P. V. Santos, arXiv:1310.3027v1 [physics.ins-det].

[14] J. Teipel, K. Franke, D. Türke, F. Warken, D. Meiser, M. Leuschner, and H. Giessen, Appl. Phys. B **77**, 245 (2003).

[15] J. M. Dudley and S. Coen, Rev. Mod. Phys. **78**, 1135 (2006).

[16] F. Meier and B. P. Zakharchenya, eds., *Optical Orientation*, Modern Problems in Condensed Matter Sciences, Vol. 8 (North-Holland, Amsterdam, 1984).

[17] A. V. Kimel, V. V. Pavlov, R. V. Pisarev, V. N. Gridnev, F. Bentivegna, and T. Rasing, Phys. Rev. B **62**, R10610 (2000).

[18] J. M. Kikkawa, I. P. Smorchkova, N. Samarth, and D. D. Awschalom, Science **277**, 1284 (1997).

[19] L. M. Smith, D. R. Wake, J. P. Wolfe, D. Levi, M. V. Klein, J. Klem, T. Henderson, and H. Morkoç, Phys. Rev. B **38**, 5788 (1988).

[20] H. Zhao, M. Mower, and G. Vignale, Phys. Rev. B **79**, 115321 (2009).

[21] M. Hruška, Š. Kos, S. A. Crooker, A. Saxena, and D. L. Smith, Phys. Rev. B **73**, 075306 (2006).

[22] J.-H. Quast, T. Henn, T. Kiessling, W. Ossau, L. W. Molenkamp, D. Reuter, and A. D. Wieck, Phys. Rev. B **87**, 205203 (2013).

[23] J. M. Kikkawa and D. D. Awschalom, Phys. Rev. Lett. **80**, 4313 (1998).

[24] $E_{ex} = (E_{photon} - E_{gap})/(1 + m_e/m_h)$. $E_{photon} = 1.590$ eV and $E_{gap} = 1.518$ eV are the pump laser photon energy and GaAs band gap, $m_e = 0.067 m_0$ and $m_h = 0.51 m_0$ denote the electron and heavy hole effective masses (m_0: bare electron mass).

[25] J. Shah and R. Leite, Phys. Rev. Lett. **22**, 1304 (1969).

[26] R. Ulbrich, Phys. Rev. B **8**, 5719 (1973).

[27] Precondition for the discussion of an electron temperature is the establishment of a thermalized, i.e. Maxwell-Boltzmann or Fermi-Dirac distributed electron population. For the 6-μW pump power and the 36.4-MHz repetition rate employed in our experiment we estimate an initial photocarrier-density of $\approx 1.5 \times 10^{17}$ cm^{-3} after the excitation pulse which significantly exceeds the doping density of our sample. Time-resolved photoluminescence studies[29] on bulk GaAs have demonstrated that the photocarrier thermalization by very efficient electron-electron scattering takes place on timescales well below 15 ps even for excitation densities two orders of magnitude lower than employed in our work. We therefore conclude that the electron ensemble is thermalized even for the shortest delays of 13 ps examined in our measurements and can be characterized by a well-defined electron temperature.

[28] R. Ulbrich, Solid-State Electron. **21**, 51 (1978).

[29]D. W. Snoke, W. W. Rühle, Y. C. Lu, and E. Bauser, Phys. Rev. Lett. **68**, 990 (1992).

[30]T. Kiessling, J.-H. Quast, A. Kreisel, T. Henn, W. Ossau, and L. W. Molenkamp, Phys. Rev. B **86**, 161201 (2012).

[31]We have verified that the temporal evolution of the $(1/e)$ half width obtained from our simulation does not depend on the exact value of the temporal width τ_g of the source term, i.e. $w_s^2(\Delta t)$ does not change when varying τ_g within our experimental time resolution.

[32]S. A. Crooker and D. L. Smith, Phys. Rev. Lett. **94**, 236601 (2005).

[33]T. Henn, A. Heckel, M. Beck, T. Kiessling, W. Ossau, L. W. Molenkamp, D. Reuter, and A. D. Wieck, Phys. Rev. B **88**, 085303 (2013).

[34]H. Hoffmann, G. V. Astakhov, T. Kiessling, W. Ossau, G. Karczewski, T. Wojtowicz, J. Kossut, and L. W. Molenkamp, Phys. Rev. B **74**, 073407 (2006).

[35]H. Münzel, A. Steckenborn, and D. Bimberg, J. Lumin. **24/25**, 569 (1981).